



Ultrasensitive mass sensor fully integrated with complementary metal-oxide-semiconductor circuitry

Forsén, Esko Sebastian; Abadal, G.; Ghatnekar-Nilsson, S.; Teva, J.; Verd, J.; Sandberg, Rasmus Kousholt; Svendsen, Winnie Edith; Perez-Murano, F.; Esteve, J.; Figueras, E.

Total number of authors:

14

Published in:

Applied Physics Letters

Link to article, DOI:

[10.1063/1.1999838](https://doi.org/10.1063/1.1999838)

Publication date:

2005

Document Version

Publisher's PDF, also known as Version of record

[Link back to DTU Orbit](#)

Citation (APA):

Forsén, E. S., Abadal, G., Ghatnekar-Nilsson, S., Teva, J., Verd, J., Sandberg, R. K., Svendsen, W. E., Perez-Murano, F., Esteve, J., Figueras, E., Campabadal, F., Montelius, L., Barniol, N., & Boisen, A. (2005). Ultrasensitive mass sensor fully integrated with complementary metal-oxide-semiconductor circuitry. *Applied Physics Letters*, 87(4), 043507. <https://doi.org/10.1063/1.1999838>

General rights

Copyright and moral rights for the publications made accessible in the public portal are retained by the authors and/or other copyright owners and it is a condition of accessing publications that users recognise and abide by the legal requirements associated with these rights.

- Users may download and print one copy of any publication from the public portal for the purpose of private study or research.
- You may not further distribute the material or use it for any profit-making activity or commercial gain
- You may freely distribute the URL identifying the publication in the public portal

If you believe that this document breaches copyright please contact us providing details, and we will remove access to the work immediately and investigate your claim.

Ultrasensitive mass sensor fully integrated with complementary metal-oxide-semiconductor circuitry

E. Forsen

Department of Micro and Nanotechnology, Technical University of Denmark, Kgs. Lyngby, DK-2800, Denmark

G. Abadal

Department of Electronic Engineering, Universitat Autònoma de Barcelona, 08193 Bellaterra, Spain

S. Ghatnekar-Nilsson

Solid State Physics and The Nanometer Consortium, University of Lund, 22362 Lund, Sweden

J. Teva and J. Verd

Department of Electronic Engineering, Universitat Autònoma de Barcelona, 08193 Bellaterra, Spain

R. Sandberg and W. Svendsen

Department of Micro and Nanotechnology, Technical University of Denmark, Kgs. Lyngby, DK-2800, Denmark

F. Perez-Murano, J. Esteve, E. Figueras, and F. Campabadal

National Microelectronics Centre, Universitat Autònoma de Barcelona, 08193 Bellaterra, Spain

L. Montelius

Solid State Physics and The Nanometer Consortium, University of Lund, 22362 Lund, Sweden

N. Barniol

Department of Electronic Engineering Universitat Autònoma de Barcelona, 08193 Bellaterra, Spain

A. Boisen

Department of Micro and Nanotechnology, Technical University of Denmark, Kgs. Lyngby, Dk-2800, Denmark

(Received 17 March 2005; accepted 7 June 2005; published online 21 July 2005)

Nanomechanical resonators have been monolithically integrated on preprocessed complementary metal-oxide-semiconductor (CMOS) chips. Fabricated resonator systems have been designed to have resonance frequencies up to 1.5 MHz. The systems have been characterized in ambient air and vacuum conditions and display ultrasensitive mass detection in air. A mass sensitivity of 4 ag/Hz has been determined in air by placing a single glycerine drop, having a measured weight of 57 fg, at the apex of a cantilever and subsequently measuring a frequency shift of 14.8 kHz. CMOS integration enables electrostatic excitation, capacitive detection, and amplification of the resonance signal directly on the chip. © 2005 American Institute of Physics. [DOI: 10.1063/1.1999838]

The advances of nanotechnology can be utilized in developing portable sensor systems for applications in biological, physical, or chemical sensing, achieving ultrasensitive detection with low analyte consumption. One approach in developing such a system is to make a nanoresonator device where a change in the mass of the resonator is detected as a change in the resonance frequency of the resonator. In order to achieve the highest possible mass sensitivity, research on fabrication, integration, and development of nanoelectromechanical resonator systems is pursued.^{1–3} The most frequently used techniques for measuring the resonance frequency of a cantilever are based on optical detection.⁴ The advantage is its inherent simplicity and high sensitivity. Some disadvantages are problems with alignment capability, miniaturization and portability. Resonator systems can be actuated by piezoelectric, magnetic, or thermal actuation.^{5–7} Another option is to use electrostatic actuation and capacitive readout. This is achieved by connecting nano/microstructures with standard microelectronics. Previously,^{8–11} we have reported on the principle of design and fabrication of cantilever resonators integrated with standard complementary metal-oxide-semiconductor (CMOS)

circuitry. CMOS integration enables simple electrostatic actuation, capacitive read-out, and signal amplification. In this letter, we present the functional evaluation of CMOS integrated cantilever structures achieving attogram/Hz mass resolution in air.

The sensing principle is based on monitoring the resonance frequency change of a cantilever as a function of mass adsorption, e.g., due to the adsorption of molecules. The nanoresonator structures are excited into lateral vibration by applying an ac and dc voltage between the suspended cantilever and a fixed parallel electrode. The frequency shift upon added mass is measured on-chip by capacitive resonance frequency detection. CMOS integration reduces the parasitic capacitance contribution and is hence crucial for our choice of cantilever readout. Furthermore, CMOS integration allows for increased functionality in terms of frequency tracking and Q -factor enhancement,^{12,13} and can be used as a component in a portable device.

The nanoresonators are defined by combined electron-beam lithography and direct write laser lithography on a preprocessed CMOS chip.¹¹ Examples of fabricated 425 nm wide, 600 nm thick, and 20 μm long polycrystalline silicon

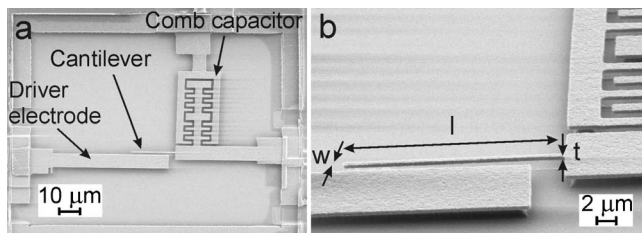


FIG. 1. SEM images of fabricated poly-Si cantilever structures on a CMOS chip. (a) Top view image of a defined cantilever structure. The cantilever is excited into lateral resonance by applying an ac and dc voltage between the driver electrode and the cantilever. The cantilever is connected to a comb capacitor in order to polarize the CMOS circuitry. (b) Tilted view image of a 20 μm long, 425 nm wide, and 600 nm thick cantilever.

(poly-Si) cantilevers, integrated on a CMOS chip, are demonstrated in Fig. 1. We have used standard CMOS technology¹⁴ which leads to cantilever design constraints, limiting the highest detectable resonance frequency to approximately 2 MHz. The on-chip frequency response of such a cantilever, as a function of applied dc voltage (V_{dc}), is measured using a gain-phase analyzer, see Fig. 2(a). The resonance frequency is reduced when the V_{dc} is increased, due to electrostatic spring softening.¹⁵ The unperturbed resonance frequency of the system is determined to be $f_0 = 1.487$ MHz from the intersection of the linear fit with the y axis at zero-applied voltage, Fig. 2(b). Electrical measurements performed on equivalent cantilevers without an integrated CMOS circuit did not show any appreciable resonance frequency signal, due to the screening effect of the parasitic capacitance introduced by the pads and external wires. The Young's modulus of the poly-Si cantilever is calculated using Eq. (1) to have a value of $E = 175 \pm 18$ GPa (Ref. 16)

$$E = \frac{16\pi^2 \ell^4 \rho n_1 f_0^2}{w^2}, \quad (1)$$

in which $\ell = 20$ μm is the length and $w = 425$ nm is the width of the cantilever, $\rho = 2.33 \times 10^6$ g/m³ is the mass density of the poly-Si, $n_1 \cong 0.2427$ is a geometrical form factor for the fundamental vibration mode originating from the Euler-Bernoulli beam equation.¹⁷ The calculated Young's modulus is consistent with measurements on similar poly-Si thin films with $E = 158 \pm 7$ GPa.¹⁸

Resonator structures have been characterized in a chamber in which the pressure has been controlled in the range of 1013 mbar–0.1 mbar. The quality factor as a function of the pressure displays a log-log dependence, as shown in Fig. 2(c). Given a dc+ac actuation voltage of 1 V_{dc} and 0.9 V_{pp} peak-peak (V_{pp}), a quality factor of approximately 5000 is determined at a pressure of 0.4 mbar. The quality factor is reduced to 30 at ambient air conditions. This is comparable to previous visual characterization of similar sized equivalent resonators that have not been CMOS integrated. Here, a quality factor of 70 was found for air operation¹⁴ and the value increased to 28 000 for operation at a pressure of 2 μmbar .⁸

In order to characterize the mass sensitivity of the resonator device in air, punctual masses are placed on the cantilever. Single glycerine drops are placed selectively on the apex of the cantilever using a glycerine coated scanning tunneling microscope (STM) tip. The deposited glycerine drop has a diameter of approximately 500 nm, estimated by com-

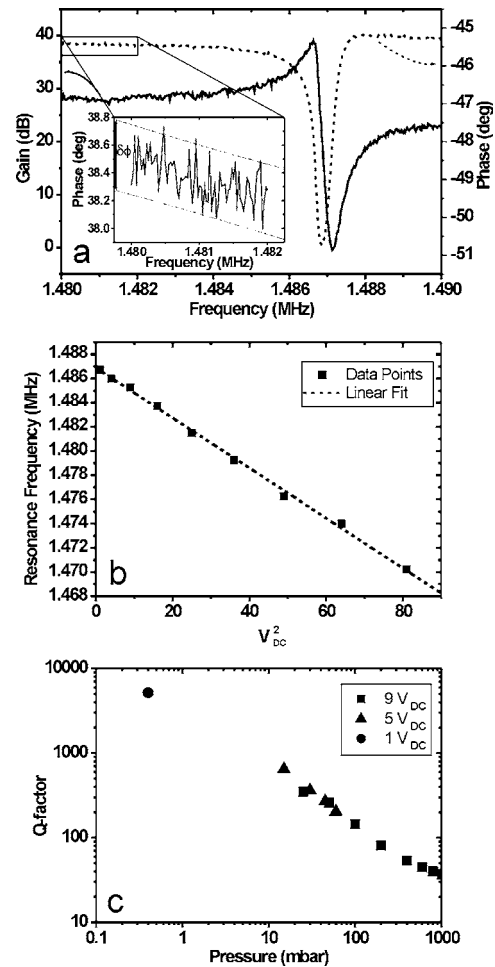


FIG. 2. (a) On-chip readout using a poly-Si cantilever with a width of 425 nm, a thickness of 600 nm and a length of 20 μm , at a pressure of 0.4 mbar. The frequency signal from the CMOS circuitry was analyzed using a gain-phase analyzer. The inset shows the fluctuation of the phase signal ($\delta\phi \approx 0.5^\circ$). (b) The effect of electrostatic spring softening is shown. The unperturbed resonance frequency of the system is determined from the intersection of the linear fit at zero-applied dc voltage. The fundamental resonance frequency is 1.487 MHz. (c) The quality factor dependence on the pressure displays a log-log relationship. A quality factor of approximately 5000 is determined at 0.4 mbar and 1 V_{dc} and 0.9 V_{pp} .

paring the drop size with the known width of the cantilever. Assuming a hemispherical volume and $\rho = 1.26 \times 10^6$ g/m³, the mass of the glycerine drop is estimated to be 41 fg. Figure 3 shows the on-chip readout before and after the controlled positioning of a single glycerine drop at the apex of the resonator. An ac voltage of 6 V_{pp} and a dc voltage of 14 V is applied to a 20 μm long, 425 nm wide, and 600 nm thick nanoresonator, similar to the resonator shown in Fig. 1(c). A resonant frequency of 1.453 MHz is measured before the deposition of the glycerine drop. Directly after the deposition of the glycerine, a frequency shift in air of $\Delta f = 14.8$ kHz is determined from the shift in phase. From the frequency shift, an added mass of 57 fg is calculated using Eq. (2)¹⁹

$$\Delta m = \frac{2m_{\text{eff}}\Delta f}{f_0}, \quad (2)$$

where $m_{\text{eff}} = n_1 \rho \ell w t$ is the effective mass of the cantilever for the fundamental vibration mode, calculated using a density of poly-Si $\rho = 2.33 \times 10^6$ g/m³, and a resonance frequency

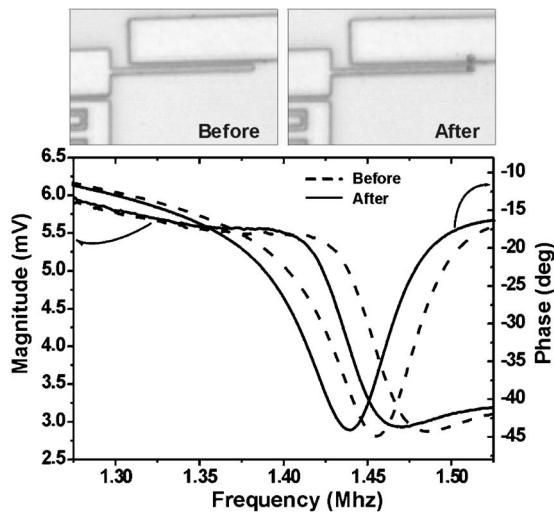


FIG. 3. The diagram shows the electrical resonance signal for a poly-Si resonator structure as measured through the CMOS. At ambient conditions, the resonance frequency was 1.453 MHz. The cantilever is 20 μm long, 425 nm wide, and 600 nm thick. The cantilever is excited into resonance by applying 14 V_{dc} and 6 V_{pp} ac. The inset shows two glycerine droplets, one at the apex of the cantilever and the other is on the parallel actuation electrode. This is due to the fact that the glycerine-coated STM-tip touched the electrode on the first approach, resulting in a glycerine drop on the electrode. After deposition of a single glycerine drop onto the cantilever, the resonance frequency was reduced by 14.8 kHz, which yields a mass sensitivity on the order of 4 ag/Hz at ambient conditions.

$f_0 = 1.487$ MHz. Hence, the calculated mass sensitivity of the system is 4 ± 1 ag/Hz.

Inevitably, the ultimate mass resolution is limited by the noise of the system. In order to get an estimate of the minimal detectable mass, δM , which is the mass change that results in a frequency shift that overcomes the noise floor, an investigation of the phase noise of the system needs to be conducted. From the inset in Fig. 2(a), the magnitude of the phase noise—caused by both intrinsic and extrinsic noise sources from the transducer and the readout circuitry—can be determined to be of the order of $\delta\phi \approx 0.5^\circ$ at a pressure of 0.4 mbar. Since the slope of the phase signal at the frequency of the resonance peak was $\partial\phi/\partial f = -0.108$, the corresponding minimum frequency shift is $\delta f \approx 4.6$ Hz. Hence, the minimal detectable mass is calculated as $\delta M_{\text{noise}} = 2m_{\text{eff}}\delta f/f_0 \approx 18$ ag. The ultimate resolution for a nanoresonator, equivalent with the one presented in this letter, only taking intrinsic phase noise into account and excluding extrinsic noise limitations can be approximated using Eq. (3):¹⁹

$$\delta M_{\text{intrinsic}} = 2m_{\text{eff}}\sqrt{E_T/E_c}\sqrt{\Delta f/Q2\pi f_0} \approx 1 \text{ ag}, \quad (3)$$

where $E_T = k_B T$ is the thermal energy at room temperature, $E_c = m_{\text{eff}}4\pi^2 f_0^2 \langle x_c^2 \rangle$ is the driving energy, $\langle x_c \rangle \approx 100$ nm is the approximate root-mean-square drive amplitude in the direction of vibration still consistent with producing a linear response, and $\Delta f = 1$ kHz is the measurement bandwidth. This is consistent with the theoretical/experimental work by Ekinci et al.^{4,19} regarding noise limitations for nanoresonator mass sensor systems.

The phase noise is increased as one increases the pressure, mainly due to the reduced quality factor but also adsorption/desorption processes on the cantilever and additional drift of the circuit are limiting factors. At ambient conditions, the minimum frequency shift that can be moni-

tored is of the order of $\delta f \approx 1$ kHz, which corresponds to an ultimate mass resolution in air of the order of a few femtograms.

In conclusion, the characterization of a fully integrated resonator mass sensor system in air and at low pressure conditions has been discussed. CMOS integrated cantilevers have been electrostatically excited into mechanical resonance and the resonance frequency has been detected on-chip by capacitive readout. The mass sensitivity of the system has been determined by controlled positioning of glycerine drops on a cantilever, whereby a mass sensitivity of the order of 4 ag/Hz is measured for a resonator system with a fundamental resonance frequency of 1.487 MHz. At 0.4 mbar, the quality factor is determined to be approximately 5000. The sensitivity of the system is comparable to recent results achieved with resonator structures based on external actuation and readout.^{4,20} Nanoresonator devices should be functionalized in order to enable selective mass sensing. The ultimate goal is to develop nanoresonator devices as integral parts of a portable sensor system.

The authors would like to acknowledge funding granted by the European Union IST project NANOMASS II (IST-2001-33068), NANOSES (MEYT-MC2003-07237), and NANOSYS (TIC2003-0723)

¹N. V. Lavrik and P. G. Datskos, Appl. Phys. Lett. **82**, 2697 (2003).

²J. Yang, T. Ono, and M. Esashi, Sens. Actuators, A **82**, 102 (2000).

³K. L. Ekinci, X. M. H. Huang, and M. L. Roukes, Appl. Phys. Lett. **84**, 4469 (2004).

⁴R. Wiesendanger, *Scanning Probe Microscopy and Spectroscopy* (Cambridge University Press, Cambridge, U. K., 1994).

⁵A. N. Cleland, M. Pophristic, and I. Ferguson, Appl. Phys. Lett. **79**, 2070 (2001).

⁶H. J. Cho and C. H. Ahn, *Proceedings of the International Conference MEMS 2000* (2000), p. 686.

⁷C. Hagleitner, A. Hierlemann, D. Lange, A. Kummer, N. Kerness, O. Brand, and H. Baltes, Nature (London) **414**, 293 (2001).

⁸Z. J. Davis, G. Abadal, B. Helbo, O. Hansen, F. Campabadal, F. Pérez-Murano, J. Esteve, E. Figueras, J. Verd, N. Barniol, and A. Boisen, Sens. Actuators, A **105**, 311 (2003).

⁹E. Forsén, S. G. Nilsson, P. Carlberg, G. Abadal, F. Pérez-Murano, J. Esteve, J. Montserrat, E. Figueras, F. Campabadal, J. Verd, L. Montelius, N. Barniol, and A. Boisen, Nanotechnology **15**, 628 (2004).

¹⁰S. Ghatnagar-Nilsson, E. Forsén, G. Abadal, J. Verd, F. Campabadal, F. Pérez-Murano, J. Esteve, N. Barniol, A. Boisen, and L. Montelius, Nanotechnology **16**, 98 (2005).

¹¹J. Verd, G. Abadal, J. Teva, M. Villaroya Gaudó, A. Uranga, X. Borrís, F. Campabadal, J. Esteve, E. Figueras Costa, F. Pérez-Murano, Z. J. Davis, E. Forsén, A. Boisen, and N. Barniol, J. Microelectromech. Syst. **14**, 508 (2005).

¹²G. Abadal, Z. J. Davis, B. Helbo, X. Borrís, R. Ruiz, A. Boisen, F. Campabadal, J. Esteve, E. Figueras, F. Pérez-Murano, and N. Barniol, Nanotechnology **12**, 100 (2001).

¹³D. Lange, C. Hagleitner, C. Herzog, O. Brand, and H. Baltes, Sens. Actuators, A **103**, 150 (2003).

¹⁴CNM-CMOS twin-well 2-poly 2-metal 2.5 micron technology.

¹⁵Z. J. Davis, G. Abadal, O. Kuhn, O. Hansen, F. Grey, and A. Boisen, J. Vac. Sci. Technol. B **18**, 612 (2000).

¹⁶The error was determined using the following measurement uncertainties: $\Delta\ell = \pm 200$ nm, $\Delta\rho = \pm 1 \times 10^5$ g/m³, $\Delta f = \pm 5$ kHz, and $\Delta w = \pm 40$ nm.

¹⁷W. T. Thomson, *Theory of Vibration with Applications*, 4th Ed. (Stanley Thornes Ltd., 1993).

¹⁸D. Maier-Schneider, A. Köpflüchli, B. S. Holm, and E. Obermeier, J. Microelectromech. **6**, 436 (1996).

¹⁹K. L. Ekinci, Y. T. Yang, and M. L. Roukes, J. Appl. Phys. **95**, 2682 (2004).

²⁰B. Ilic, H. G. Craighead, S. Krylov, W. Senaratne, C. Ober, and P. Neuzil, J. Appl. Phys. **95**, 3694 (2004).